

## B. 研究方法

- 1) ロドプシン遺伝子 P23H, S334ter 各変異ラット、RCS ラット、対照群として Sprague-Dawley (SD) ラットおよび Brown Norway (BN) ラットからそれぞれ網膜を摘出し、ホモジェナイズした。ホモジェネートから細胞分画法により可溶画分とミトコンドリア画分を調整し、各画分中の calpain 活性とタンパク質としての発現量を測定した。
- 2) calpain 活性は Succ-Leu-Tyr-AMC を基質として酵素反応を行わせることにより測定した。
- 3) calpain のタンパク質発現量は抗 calpain 抗体を用いたウエスタンブロット法にて半定量的に検索した。
- 4) ニルバジピン投与と網膜の摘出： 既報 1) にしたがって、生後 3 週齢の RCS ラットにニルバジピンを連日 2 週間腹腔内に投与した。対照群には基剤のみ投与した。投与 2 週後に屠殺し網膜を摘出した。
- 5) 摘出した網膜をホモジェナイズし、細胞分画法により可溶画分とミトコンドリア画分を調整し、各画分中の calpain 活性とタンパク質発現量を測定した。

## C. 研究結果

- 1) SD ラットと BN ラット網膜可溶画分の calpain 活性に比べ、P23H ラット (2 倍)、S334ter ラット (3 倍) および RCS ラット (5 倍) と有意に calpain 活性が上昇していた。ミトコンドリア画分では P23H ラットは SD ラットと BN ラットと有意差はみられなかったが、S334ter ラット (2.5 倍) と RCS ラット

(2.5 倍) では有意に calpain 活性が上昇していた。

- 2) 網膜 calpastatin 発現量では RCS ラットは生後 3 週齢では SD ラットと有意差をみとめないが、4 週齢、5 週齢と進むにつれ、calpastatin 量が減少することが明らかになった。
- 3) ニルバジピン投与後の RCS ラット網膜における calpain 活性は可溶画分には有意差がなかったが、ミトコンドリア画分では対照群に比し、活性と発現量が有意に低下していた。

## D. 考察

以上の結果から、ラット網膜変性モデルでは網膜変性が存在する組織では calpain 活性が野生型に比べ有意に高値を示し、細胞死に calpain が関与している可能性が示唆された。また、RCS ラットでは網膜変性の進行にともなって calpastatin の発現量も低下しており、これが calpain 活性を高めている可能性も考えられた。RCS ラットに対するニルバジピン投与は網膜ミトコンドリア画分の calpain 活性を低下させ、これがアポトーシスを抑制している可能性も考えられた。今後のさらなる検討を要するものと考えられる。

## E. 結論

RCS ラットにニルバジピンを全身投与すると、網膜ミトコンドリア画分の calpain 活性が上昇する。同時に calpain の発現量も増加することも確認された。ニルバジピン投与により RCS ラット網膜でのアポトーシスが calpain を介して疎外されている可能性が示唆された。

- F. 健康危険情報           なし
- G. 研究発表
1. 論文発表
1. Ohguro H, Shimokawa R, Ohguro I, Ishikawa F, Yamazaki H, Nakazawa M: Clinical significance of the ankle-brachial index (ABI) and pulse wave velocity (PWV) in ocular vascular diseases. *Hirosaki Medical J* 57: 65-70, 2006.
  2. Ohguro I, Ohguro H, Ohkuro H, Nakazawa M: Optic disc characteristics assessed by evaluation by clinical optic disc photographs in patients with glaucoma. *Hirosaki Med J* 57(1): 27-34, 2006.
  3. Ito T, Ohguro H, Ohguro I, Mamiya K, Nakazawa M: Effects of anti-glaucoma drops on MMP and TIMP balance in conjunctival and subconjunctival tissue. *Invest Ophthalmol Vis Sci* 47 (3): 823-830, 2006.
  4. Ishikawa F, Ohguro H, Sato S, Sato M, Yamazaki H, Nakazawa M: A case of idiopathic retinal vasculitis, aneurysm, and neuroretinitis effectively treated by steroid pulse therapy. *Jpn J Ophthalmology* 50: 181- 185, 2006.
  5. Ohguro I, Ohguro T, Ohta T, Nakazawa M.: A case of normal tension glaucoma associated with Buerger's disease. *Tohoku J Exp Med* 209(1): 49-52, 2006.
  6. Takaya K, Suzuki Y, Nakazawa M: Massive hemorrhagic retinal detachment during radial optic neurotomy. *Graefes Arch Clin Exp Ophthalmol.* 244(2): 265-267, 2006.
  7. Takaya K, Suzuki Y, Nakazawa M: Four cases of hypotony maculopathy caused by traumatic cyclodialysis treated by vitrectomy, cryotherapy, and gas tamponade. *Graefes Arch Clin Exp Ophthalmol.* 244(7): 855-858, 2006.
  8. Taira K, Nakazawa M, Takano Y, Ohta T: A case of acute zonal occult outer retinopathy in a fellow eye 5 years after presenting punctate inner choroidopathy in one. *Graefe's Arch Clin Exp Ophthalmol.* 244(7): 880-882, 2006.
  9. Terada N, Ohno N, Ohguro H, Nakazawa, M: Immunohistochemical detection of phosphorylated rhodopsin in light-exposed retina of living mouse in vivo cryotechnique. *J Histochem Cytochem.* 47:479-486, 2006.
  10. Ishikawa F, Ohguro H, Ohguro I, Yamazaki H, Mamiya K, Metoki T, Ito T, Yokoi Y, Nakazawa M: Study of light-stress effects on retinal

functions and morphology in normal and retinal degeneration in rats. Invest Ophthalmol Vis Sci (in press).

11. Taira K, Nakazawa M, Sato M: A mutation (c. 1142 del G) in the PRPF31 gene in a family with autosomal dominant retinitis pigmentosa (RP11) and its implications. Jpn J Ophthalmol (in press).

## 2. 学会発表

1. 石川 太、中澤 満、他：正常および網膜変性ラットへの光ストレスの影響 第110回日本眼科学会総会 平成18年4月13日、大阪
2. 鈴木 香、鈴木幸彦、中澤 満：ポリマー状脈絡膜血管症による多量の両眼性黄斑血腫によるt-PA併用硝子体手術経験。第110回日本眼科学会総会 平成18年4月13日、大阪
3. 平 紅、中澤 満：涙腺癌に対する眼窩内容除去術と眼科再建術の検討 第110回日本眼科学会総会 平成18年4月13日、大阪
4. 伊藤 忠、中澤 満、他：イソプロピルウノプロストン点眼液の網膜保護効果についての検討。第110回日本眼科学会総会 平成18年4月13日、大阪

## H. 知的財産権の出願・登録状況

1. 特許取得 なし
2. 実用新案登録なし
3. その他 なし

## I. 参考文献

Yamazaki H, et al: Invest Ophthalmol Vis Sci 43(4): 919-926, 2002.

# Prolonged Rhodopsin Phosphorylation in Light-Induced Retinal Degeneration in Rat Models

Futoshi Ishikawa,<sup>1</sup> Hiroshi Ohguro,<sup>2</sup> Ikuyo Ohguro,<sup>2</sup> Hitoshi Yamazaki,<sup>1</sup> Kazubisa Mamiya,<sup>1</sup> Tomomi Metoki,<sup>1</sup> Tadashi Ito,<sup>1</sup> Yumiko Yokoi,<sup>1</sup> and Mitsuru Nakazawa<sup>1</sup>

**PURPOSE.** The effects of various light-induced stresses on the retina were examined in the retinal degenerative rat model.

**METHODS.** Retinal morphology and electroretinograms (ERGs) were analyzed after application of light-induced stress of several intensities (650, 1300, 2500, or 5000 lux). For evaluation of rhodopsin (Rho) function, the kinetics of Rho regeneration and dephosphorylation were studied by spectrophotometric analysis and immunofluorescence labeling with antibodies specifically directed toward the phosphorylated residues <sup>334</sup>Ser and <sup>338</sup>Ser in the C terminus of Rho. Retinal cGMP concentration was determined by ELISA. Expression levels of neurotrophic factors (FGF2, brain-derived neurotrophic factor [BDNF], platelet-derived growth factor [PDGF], and ciliary neurotrophic factor [CNTF]) were evaluated quantitatively by RT-PCR.

**RESULTS.** Light intensity-dependent deterioration of ERG responses and thinning of the retinal outer nuclear layer were observed in wild-type and Royal College of Surgeons (RCS) rat retinas. Under dark adaptation after light-induced stress, the kinetics of Rho regeneration were not different between wild-type and RCS rat retinas. Rho dephosphorylation at <sup>334</sup>Ser and <sup>338</sup>Ser was extremely delayed in RCS rat retinas compared with wild-type without light-induced stress, but Rho dephosphorylation at those sites became slower in both RCS and wild-type rat retinas. In terms of expression of neurotrophic factors, almost no significant changes were observed between the animals after light-induced stress.

**CONCLUSIONS.** The present study indicates that light-induced stress causes intensity-dependent deterioration in retinal function and morphology in wild-type and RCS rat retinas. Disruption of the phototransduction cascade resulting from slower kinetics of Rho dephosphorylation appears to be involved in retinal degeneration. (*Invest Ophthalmol Vis Sci.* 2006;47:5204-5211) DOI:10.1167/iovs.05-1149

**R**etinitis pigmentosa (RP) is a heterogeneous disease group of progressive hereditary retinal degeneration clinically characterized by night blindness, visual field defects, and ab-

normal electroretinogram (ERG) responses due to photoreceptor cell death.<sup>1</sup> Mutations of retinal genes,<sup>1</sup> light damage,<sup>2</sup> and autoimmune responses<sup>3</sup> are all involved in photoreceptor cell death. Several animal models with gene deficits and in vivo retinal cell death induced by intense light-induced stress<sup>2</sup> or intravitreal administration of antibodies<sup>3</sup> have been developed recently. Among these, the Royal College of Surgeons (RCS) rat, in which the retinal pigment epithelium (RPE) cell is affected by the gene encoding the receptor tyrosine kinase *Mertk* has been the most widely used in the study of RP. In terms of the cause of retinal degeneration in this rat, it has been suggested that an inability of the shed tips to perform phagocytosis of rod outer segment (ROS) debris by RCS RPE is primarily involved.<sup>4-6</sup> Nir et al.<sup>7,8</sup> described an interesting observation that light-induced stress promotes photoreceptor cell survival and function in the RCS rat, whereas light-induced stress causes apoptotic cell death in wild-type and other types of animal models with retinal degeneration. As a possible mechanism of the light-induced protective mechanism in the RCS rat retina, they suggested that light-induced stress may enhance the levels of expression of FGF2, which has been shown to be a possible survival factor of RCS retinal degeneration.<sup>7,8</sup> This beneficial effect toward RCS retinal degeneration suggests that some modulation in functions of the photoreceptor outer segment (OS) by light exposure must be related, because it is the only receptor for light within retinal neurons, and light triggers the visual transduction cascade reactions within OS. Therefore, to elucidate what kinds of mechanisms are involved on light-induced stress, systematic studies of photoreceptor cell functions including each step of the visual transduction processes, photoexcitation, quenching, and adaptation are essentially required.

To gain new insights into the mechanism of light-induced stress on RCS retinal degeneration, we exposed RCS and wild-type rats to various illumination conditions, and the resultant retinal function was evaluated by ERG, rhodopsin (Rho) regeneration, Rho phosphorylation, cGMP concentration, and morphologic analysis. In addition, mRNA expression levels of several neurotrophic factors were investigated.

## MATERIALS AND METHODS

All experimental procedures were designed to conform to the ARVO Statement for Use of Animals in Ophthalmic and Vision Research and our own institution's guidelines. Unless otherwise stated, all procedures were performed at 4°C or on ice in ice-cold solutions.

### Light-Induced Stress Conditions to Wild-Type (SD, BN) Rats and Retinal Degeneration (RCS) Rats

In the present study, 3- to 5-week-old Sprague-Dawley (SD) rats, Brown Norway (BN) rats (Crea, Tokyo, Japan) and 3- to 5-week-old inbred RCS (*rdy*<sup>-/-</sup>) rats (albino type; Crea) reared in cyclic light conditions (650 lux, 12 hours on-off) were used. SD, BN, or RCS rats were exposed to 650, 1300, 2500, and 5000 lux white light for 24 hours in a light-induced stress box equipped with white fluorescent lamps and cov-

From the <sup>1</sup>Department of Ophthalmology, Hirosaki University School of Medicine, Hirosaki, Japan; and the <sup>2</sup>Department of Ophthalmology, Sapporo Medical University School of Medicine, Sapporo, Japan.

Supported by grants from the Japanese Ministry of Health and Welfare and by a Grant-in-Aid for Scientific Research from the Japanese Ministry of Education, Sports and Culture.

Submitted for publication August 28, 2005; revised January 24, March 25, and July 4, 2006; accepted October 23, 2006.

Disclosure: F. Ishikawa, None; H. Ohguro, None; I. Ohguro, None; H. Yamazaki, None; K. Mamiya, None; T. Metoki, None; T. Ito, None; Y. Yokoi, None; M. Nakazawa, None

The publication costs of this article were defrayed in part by page charge payment. This article must therefore be marked "advertisement" in accordance with 18 U.S.C. §1734 solely to indicate this fact.

Corresponding author: Hiroshi Ohguro, Department of Ophthalmology, Sapporo Medical University School of Medicine, S1W17, Chuo-ku, Sapporo 060-8556, Japan; ooguro@sapmed.ac.jp.

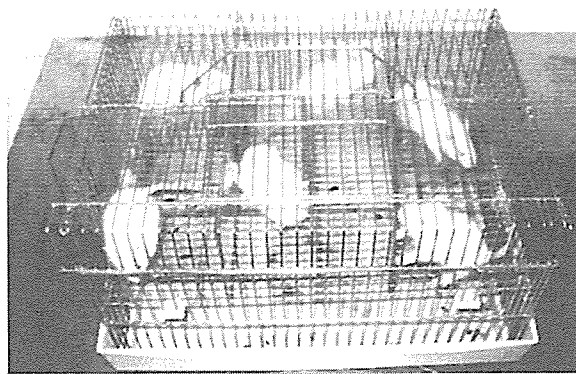
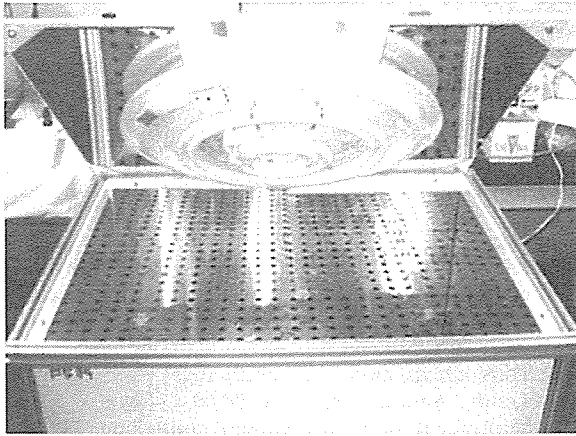


**FIGURE 1.** Light-induced stress for normal and RCS rats. Light-induced stress was administered to wild-type and RCS rats using a light-induced stress box. Inner walls of the light-induced stress box are all covered by mirrors, and white fluorescence lights are attached under the top cover by which the light intensity can be controlled (*top*). Six rats could be housed in a cage which was divided into six rooms by acrylic boards to keep the rats separate (*bottom*). The luminance levels differed less than 3% among each of the boxes within the cages.

ered inside by mirrors (Fig. 1). The rats were kept under usual cyclic light conditions or dark adaptation for ERG measurement and histologic examination. ERG measurements were performed at 1, 7, and 30 days in SD and BN rats, and 1 and 7 days in RCS rats after light-induced stress. Histologic examination was performed at 7 and 60 days in SD and BN rats and at 7 days in RCS rats after the light-induced stress.

### ERG Measurement

Details of the preparation, recording technique, and measurements of ERG have been described elsewhere.<sup>9</sup> Before ERG measurement, rats were subjected to 24 hours of dark adaptation. Under anesthesia, the each rat was laid on its side with its head fixed in place with surgical tape in an electrically shielded room for overnight dark adaptation. The pupils were dilated with drops of 0.5% tropicamide. ERGs were recorded with a contact electrode equipped with a suction apparatus to fit on the cornea (Kyoto Contact Lens Co., Kyoto, Japan). A ground electrode was placed on the ear. Responses evoked by white flashes ( $3.5 \times 10^2$  lux, 200-ms duration) using a Ganzfeld dome (SG-2002; Meiyo Co., Tokyo, Japan) were recorded and studied with ERG-analysis software (PowerLab Scope version 3.7; ADInstruments Ltd., Castle Hill, NSW, Australia). The a-wave amplitude was determined from the baseline to the bottom of the a-wave. The b-wave amplitude was determined from the bottom of the a-wave to the top of the b-wave.

### Preparation of Specific Antibodies toward Phosphorylated Rho at 334Ser or 338Ser

Specific antisera toward phosphorylated Rho at <sup>334</sup>Ser or <sup>338</sup>Ser were obtained by immunization of phosphorylated authentic peptides P-Rho334 peptide (DDEApSATASK) or P-Rho338 peptide (CEASATApSKT) chemically conjugated with bovine thyroglobulin, and antisera were each further purified into IgG by protein G Sepharose column chromatography as described recently.<sup>10</sup> Each purified antibody (0.1 mg IgG) was then incubated with urea-washed rat ROS (20 mg) at room temperature for 2 hours, and then the mixture was ultracentrifuged at 100,000g for 1 hour. The resultant supernatant was used as a specific antibody toward phosphorylated Rho at <sup>334</sup>Ser or <sup>338</sup>Ser. Antibody titers and their specificities were determined by ELISA and Western blot, respectively, as described in our recent report.<sup>10</sup>

### Light and Immunofluorescence Microscopy

Enucleated eyes were fixed with methacarn (60% methanol, 30% chloroform, 10% glacial acetic acid) overnight, dehydrated, and embedded in paraffin. Posterior segments cut from the enucleated eyes were embedded in paraffin. Retinal sections were cut vertically through the optic disc at 2- $\mu$ m thickness, mounted on subbed slides, and dried. The sections were processed with hematoxylin-eosin staining after deparaffinization with graded ethanol and xylene solutions. For evaluation of photoreceptor cell survival, the sections including the full length of the retina from the optic nerve head through the ora serrata were photographed, and the rows of cell nuclei in the photoreceptor outer nuclear layer (ONL) were counted at 200- $\mu$ m intervals along the whole horizontal retinal axis.

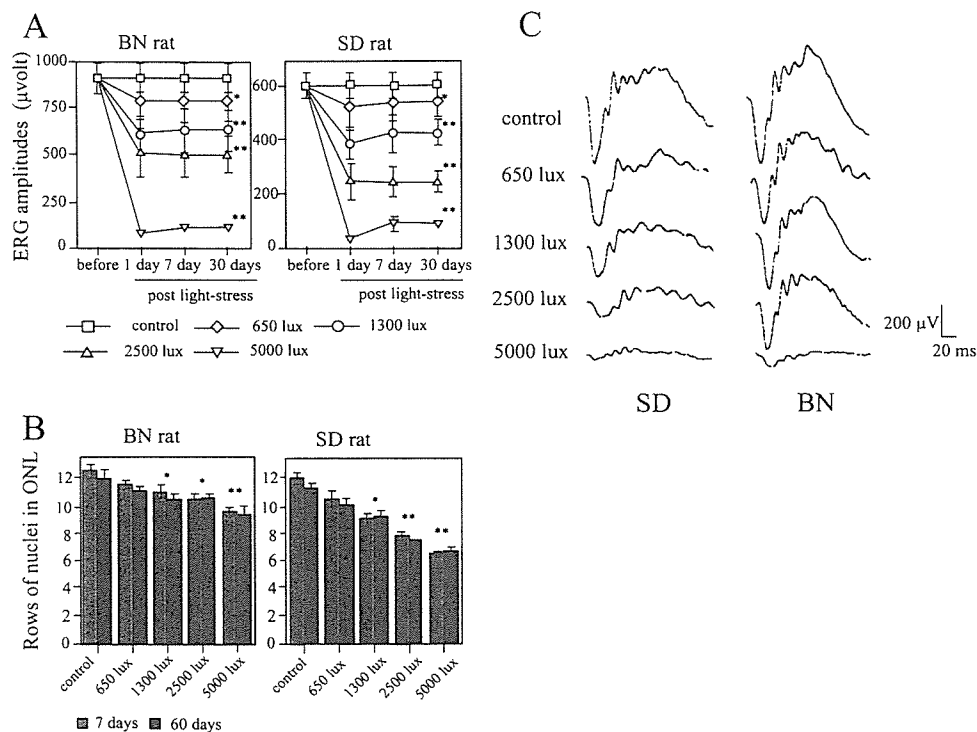
For immunofluorescence labeling, after the deparaffinization, sections were blocked with phosphate-buffered saline (PBS) containing 5% goat serum and 3% bovine serum albumin (BSA) for an hour and then incubated overnight with anti-P-Rho334 peptide antibody or anti-P-Rho338 peptide antibody (1:500) at 4°C. Sections were washed and incubated with fluorescein-isothiocyanate (FITC)-conjugated antibodies to rabbit IgG (Cappel, Durham, NC) for an hour at room temperature. Specificity controls were obtained by omitting the primary antibodies. Sections were observed, and pictures were taken with a fluorescence microscope (model BH-2; Olympus, Tokyo, Japan) using a blue filter.

### Quantitative RT-PCR Analysis

Total RNA from retinas (four eyes, two rats were used in each experimental condition) was isolated (Isogen Reagent) according to the procedure recommended by the manufacturer (Nippon gene, Tokyo, Japan). The cDNAs were generated from 2  $\mu$ g retinal RNA in a 12- $\mu$ L reaction with 1  $\mu$ L oligo(dT) primer (0.5 mg/mL; Invitrogen-Gibco, Rockville, MD). The reaction mix was denatured at 70°C for 10 minutes. Four microliters of first-strand buffer (250 mM Tris-HCl, 375 mM KCl, 15 mM MgCl<sub>2</sub>; Superscript; Invitrogen-Gibco), 2  $\mu$ L dithiothreitol (0.1 M; DTT; Invitrogen-Gibco), 1  $\mu$ L deoxyribonucleoside triphosphate (10 mM; dNTP; Invitrogen-Gibco), 1  $\mu$ L RNase inhibitor (40 U/ $\mu$ L; RNase inhibitor; Invitrogen-Gibco), and 1  $\mu$ L reverse transcriptase (200 U/ $\mu$ L; Superscript II; Invitrogen-Gibco) were added to the mixture. The incubation was performed at 42°C for 50 minutes and at 70°C for 15 minutes. The PCR amplifications were performed using 4  $\mu$ L from the RT reaction, 5  $\mu$ L 10 $\times$  PCR buffer (200 mM Tris-HCl, 500 mM KCl), 2  $\mu$ L MgCl<sub>2</sub> (50 mM), 1  $\mu$ L dNTP, 5  $\mu$ L sense and antisense primers (10 pM/ $\mu$ L), and 0.5  $\mu$ L *Taq* polymerase (5 U/ $\mu$ L; Invitrogen-Gibco). The PCR mixture was denatured at 94°C for 4 minutes and then run for 30 cycles of 94°C for 1 minute, 55°C for 1 minute, and 72°C for 2 minutes.

For PCR analysis (*Taqman*; Applied Biosystems, Inc. [ABI], Foster City, CA), the primers and probes were designed on computer (Primer-Express software; ABI) as follows:

*FGF2* (Gene ID 54250) forward, 5'-28CGCACCTATCCCCTCACAC-3', reverse, 5'-128TCCACCCAAAGCAGTAGAAGGA-3', detection probe, 5'-73TCCAAACCTGACCCGATCCCTCC-3'.



and (B), respectively. (C) Representative ERGs obtained from rats exposed to light-induced stress with several light intensities at 1 day after exposure. \* $P < 0.01$ , \*\* $P < 0.001$  (Mann-Whitney test).

*CNTF* (Gene ID 25707) forward, 5'-78ATGGCTTTCGACAGCAAA-3', reverse, 5'-262TCAGTGCTTGCCACTGGTACA-3', detection probe, 5'-102CTGACCCTTACCGCCGGGA-3'.

*BDNF* (Gene ID 24225) forward, 5'-254CAAGCCACCATCAAAAGACTGA-3', reverse, 5'-333GCTTGCCGGTTCCTCTCTCT-3', detection probe, 5'-292ACAAGCGGCGGCACTTCCTCG-3'.

*PDGF* (Gene ID 25266) forward, 5'-307TGACAGCCTCCCTGACT-3', reverse, 5'-376CACCTGATTGAACCTGCAC-3', detection probe, 5'-329AGCCTCGCTTCCACCTCCACACA-3'.

Rodent *GAPDH* as an internal control was amplified by using a commercially available kit (ABI) at the same time. The PCR mix contained 1  $\mu$ L cDNA template; 1  $\times$  Taqman buffer A 8% glycerol; 5 mM MgCl<sub>2</sub>; 200  $\mu$ M each of dATP, dCTP, and dGTP; and 400  $\mu$ M dUTP; 1.25 units DNA polymerase (AmpliTaQ Gold; ABI), 0.25 units uracil-N-glycosylase (AmpErase; ABI), 300 nM each of the primers in total 50  $\mu$ L. Standard reactions were performed with a sequence detection system (Prism; ABI). All experiments were performed in triplicate.

## Other Analytical Methods

Rho regeneration was determined by spectrophotometric analysis, as described previously.<sup>11</sup> Briefly, rats were exposed to the different illumination intensities as described earlier and then subjected to dark adaptation. At different times during dark adaptation, under dim red light, rats were euthanized, and eyes were enucleated and halved into the anterior and posterior segments. The posterior segments were then homogenized with 10 mM HEPES buffer (pH 7.5), containing 10 mM dodecyl  $\beta$ -maltoside and 20 mM hydroxylamine by a glass-glass homogenizer. The sample was centrifuged at 20,000g, and the spectra were recorded before and after complete bleaching. Rho concentrations were determined from the light-sensitive OD at 498 nm, assuming a molar extinction coefficient of 40,600 at 498 nm. Retinal cytosolic cGMP concentrations were determined by ELISA kit (Assay Designs, Inc., Ann Arbor, MI), with retinal extracts used according to the manufacturer's protocol.

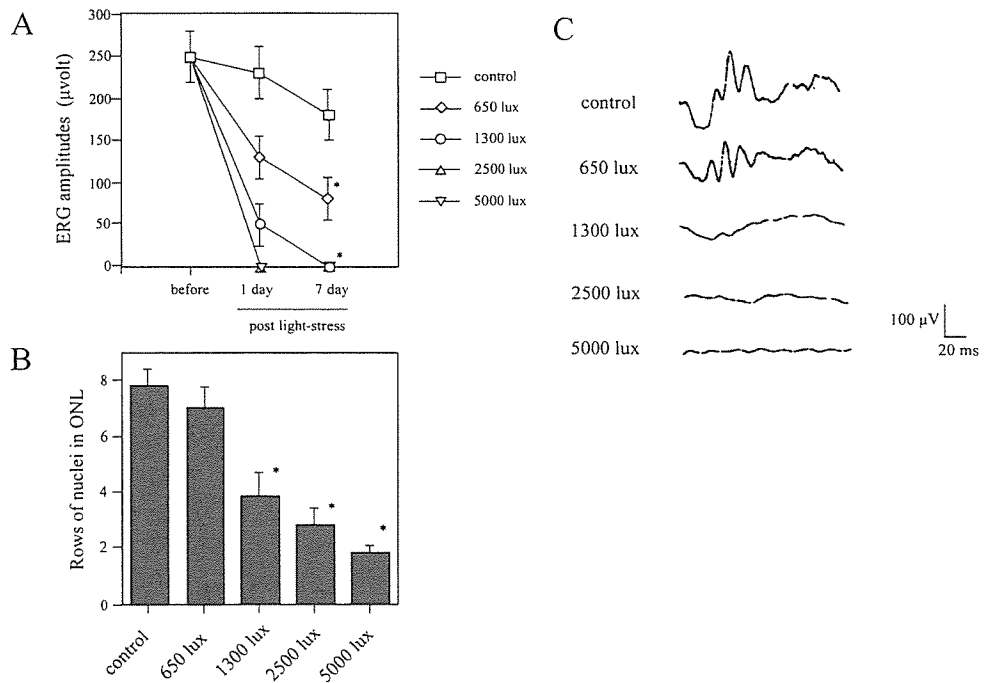
**FIGURE 2.** Effects of light-induced stress with several light intensities toward ERG responses (A) and retinal morphology (B) in BN and SD rats. Three-week-old BN or SD rats were exposed to light-induced stress with several light intensities (650, 1300, 2500, or 5000 lux) for 24 hours. Fifty rats were used in each experimental condition. After the light-induced stress, 10 rats were immediately subjected to 24 hours of dark adaptation, followed by ERG measurement. Another 10 rats were raised in regular cyclic light conditions (12 hours in 650 lux and 12 hours in the dark) for 6 or 29 days and then kept in the dark for 24 hours, followed by ERG measurements. The remaining 10 rats were kept in regular cyclic light conditions for 7 or 60 days and then euthanized. The eyes ( $n = 10$ , from 10 rats) were enucleated, the retinas were processed for hematoxylin-eosin [HE] staining of paraffin sections, and the ONL nuclei were counted. Rats raised in cyclic light conditions without light-induced stress were used as control subjects. Mean  $\pm$  SD of ERG amplitudes (b-wave) and rows of ONL nuclei are plotted in (A)

## RESULTS

An intensity-dependent deterioration of the ERG response was observed the day after light-induced stress in SD and BN rats, when the wild-type rat species were exposed to several intensities of light (650, 1300, 2500, or 5000 lux for 24 hours; Fig. 2A). Such ERG impairment was not significantly changed during the following 7 days or 30 days (Fig. 2A). Although no significant changes in retinal morphology were observed until a few days after the illumination, intensity-dependent thinning of the ONL was recognized as early as 1 week after light-induced stress (Fig. 2B). Further deterioration in the retinal morphology was not observed until 2 months after exposure to light (Fig. 2B). Similarly, retinal ONL thinning and lowering of ERG responses were detected in the RCS rat, and thereafter the ERG responses continued to decrease (Fig. 3). However, the rates of change after exposure to 650 and 1300 lux were almost identical with those of control conditions. These data indicate that intensity-dependent bright-light-induced ERG impairment was simply added to the RCS-dependent ERG deterioration. Light-induced retinal rescue effects proposed by Nir et al.<sup>7,8</sup> and other additional effects were not detected.

Next, to get insight into which steps in the phototransduction cascade were affected by such light-induced stress within photoreceptor cells, Rho regeneration and Rho dephosphorylation and cytosolic cGMP concentrations were evaluated. These factors are known to be involved in the following mechanisms: (1) initial photoreception by Rho, (2) a critical step of quenching the photoexcitation, and (3) resultant metabolite of the final steps of the vertebrate phototransduction cascade. As shown in Figure 4, rates of Rho regeneration during dark-adaptation from different light-induced bleaching conditions (1300 or 2500 lux) were almost identical in 3-week-old RCS and SD rats, suggesting that light-induced stress does not affect Rho regeneration in wild-type and RCS rats. Next, the effects of light-induced stress on Rho phosphorylation and dephosphor-

**FIGURE 3.** Effects of light-induced stress with several light intensities toward ERG responses (A) and retinal morphology (B) in RCS rats. Three-week-old RCS rats were exposed to light-induced stress with several light intensities (650, 1300, 2500, or 5000 lux) for 24 hours. Thirty rats were used in each experimental condition. After the light-induced stress, 10 rats were immediately subjected to 24 hours of dark adaptation, followed by ERG measurements. Another 10 rats were raised in regular cyclic light (12 hours in 650 lux and 12 hours in the dark) for 6 days and then kept in the dark for 24 hours followed by ERG measurements. The remaining 10 rats were kept in regular cyclic light conditions for 7 days and then euthanized. The eyes ( $n = 10$ , from 10 rats) were enucleated, the retinas were processed for HE staining of paraffin-embedded sections, and the ONL nuclei were counted. Rats raised in cyclic light conditions without light-induced stress were used as control subjects. (A–C) ERG data are as described in Figure 2. \* $P < 0.001$  (Mann-Whitney test).



ylation were studied by means of a recently developed immunohistochemical method involving a specific antibody against phosphorylated  $^{334}\text{Ser}$  or  $^{338}\text{Ser}$ , both of which have been identified as major sites of phosphorylation in Rho in vivo.<sup>14</sup> In SD rat retina,  $^{338}\text{Ser}$  antibody specifically recognized ROS of

light-adapted but not of dark-adapted retina. The immunopositivity then gradually diminished from base to tip of the ROS after dark adaptation (Fig. 5A). The  $^{334}\text{Ser}$  antibody showed identical immunolabeling properties, except that its immunoreactivity took a longer time to be diminished. Estimation of the kinetics of dephosphorylation of phosphorylated  $^{334}\text{Ser}$  and  $^{338}\text{Ser}$  sites of BN and SD were determined by measuring the vertical lengths of immunofluorescence-labeled ROS during the dark adaptation before and after the light-induced stress. Dephosphorylation of  $^{334}\text{Ser}$  and  $^{338}\text{Ser}$  sites went to completion within 1 or 2 hours and 3 or 4 hours in BN and SD rats, respectively, without light-induced stress, and dephosphorylation of these sites was significantly prolonged by light-induced stress (1300 lux; Fig. 5B). To evaluate the influence of light-induced stress on Rho dephosphorylation kinetics, the times necessary to reach 50% dephosphorylation at these phosphorylation sites during dark adaptation were determined under several conditions, as indicated in Table 1. Kinetics of Rho dephosphorylation were significantly delayed in RCS rats compared with wild-type rats, as described previously,<sup>10</sup> and those in wild-type and RCS rats were markedly delayed in a light-intensity-dependent manner.

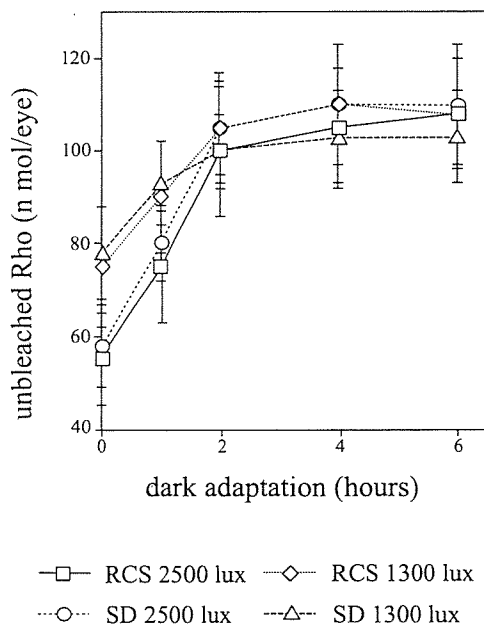


**FIGURE 4.** Time course of Rho regeneration after stress induced by light several intensities. Three-week-old SD or RCS rats treated with 1300 or 2500 lux for 24 hours were then kept in the dark. In our RCS rat strain, retinal morphology and Rho concentrations were almost comparable, although ERG responses had already deteriorated within 3 weeks after birth. At several time points—0, 1, 2, 4, and 6 hours—rats were euthanized, and enucleated eyes were processed to direct Rho concentration analysis. For each analysis, both eyes were used from one rat. Experiments were performed in triplicate using fresh preparations. No difference was observed between RCS and SD rats ( $P > 0.05$ , Mann-Whitney test). Data are expressed as the mean  $\pm$  SD.

Levels of retinal cytosolic cGMP in the SD rat were significantly decreased by light exposure compared with that in dark adaptation. In contrast, light-dependent reduction in cytosolic cGMP was less in the RCS and SD rats pretreated with exposure to bright light (1300 lux) for 24 hours (Fig. 6).

Several neurotrophic factors, including FGF2, platelet derived growth factor (PDGF), brain-derived neurotrophic factor (BDNF), and ciliary neurotrophic factor (CNTF) and other factors are known to protect both the animal model of inherited retinal degeneration and light-induced retinal damage. Nir et al.<sup>7,8</sup> recently reported that some neurotrophic factors may be involved in light-induced rescue from RCS retinal degeneration. To test whether these phenomena take place, quantitative RT-PCR was performed. However, statistically significant changes were not observed in FGF2, PDGF, or CNTF on light-induced stresses with several light intensities between RCS and SD rats during the 7 days after light-induced stress.

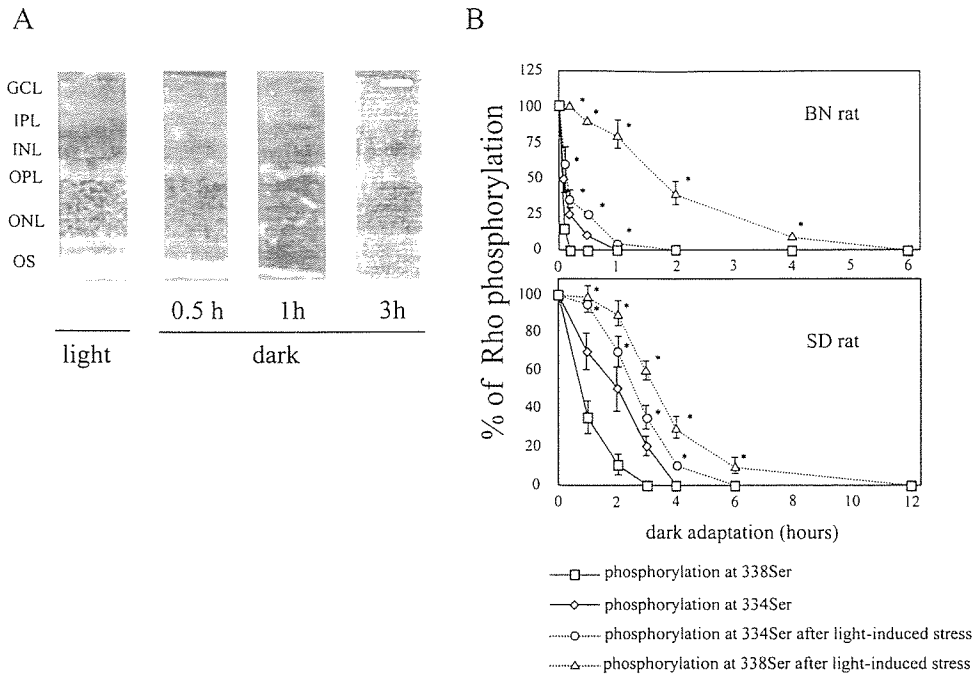


**FIGURE 5.** Kinetics of dephosphorylation in phosphorylated 334<sup>Ser</sup> and 338<sup>Ser</sup> sites in BN and SD rats pretreated by light-induced stress. Three-week-old BN or SD rats were exposed to light-induced stress (1300 lux) for 24 hours and then were maintained in the dark. At different time points (BN rats at 0, 0.1, 0.2, 0.5, 1, 2, 4, and 6 hours; SD rats at 0, 1, 2, 3, 4, 6, and 12 hours), three rats (three eyeballs) in each category were subjected to immunofluorescence labeling by anti-P-Rho antibodies. Photographs of the sections were taken. Representative photographs of SD rat retinas under light (650 lux) or after different intervals of dark adaptation were treated by anti-P-Rho 338 antibody (A). Vertical length of photoreceptor outer segment layers and that of fluorescence labeling were measured at temporal points 1.0 mm apart from optic disc from six different points from three different eyeballs and their ratios were plotted in (B). Data are expressed as the mean ± SD. GCL, ganglion

cell layer; IPL, inner plexiform layer; INL, inner nuclear layer; OPL, outer plexiform layer; ONL, outer nuclear layer; OS, outer segment. Scale bar, 25 μm. \*P < 0.01, Mann-Whitney test.

**DISCUSSION**

Light-induced stress on the retina causes a series of reactions that lead to apoptotic cell death of photoreceptors.<sup>2</sup> Its severity depends on the light's intensity, duration of exposure, and wavelength,<sup>12-14</sup> as well as the animal species, such as albino and pigmented.<sup>15</sup> Alternatively, it has also been reported that light exposure of the retina in some conditions causes protective effects against retinal photoreceptor apoptosis.<sup>7,8</sup> This beneficial effect by light exposure may be the result of light-induced stimulation for the expression of some trophic factor such as FGF2. However, the molecular mechanisms causing this response to exposure to light, which includes both destructive and beneficial effects, are controversial and have not been fully clarified. Therefore, to elucidate what kinds of mechanisms are involved in this phenomenon, we systematically studied the effects of light-induced stress of several inten-

sities on wild-type (SD and BN) and retinal degenerative (RCS) rat retinas and made the following observations: (1) On light-induced stress, intensity-dependent deterioration in retinal function analyzed by ERG and thickness of ONL occurred in wild-type rats, whereas levels of such light-induced deterioration in retinal function and morphology were different between SD (albino) and BN (pigmented) species, as described by Iseli et al.<sup>15</sup> (2) Similarly, deterioration in ERG response and retinal ONL thickness were observed in the RCS rat, but no beneficial effects on light-induced stress were observed. (3) Kinetics of Rho regeneration after light-induced stress was completed within approximately 2 hours of dark-adaptation in both wild-type and RCS rats. (4) The kinetics of Rho dephosphorylation was commonly delayed in wild-type and RCS rat retina by light-induced stress. However, these changes in kinetics exclusively depended on the rat species: albino, pigmented, and retinal degeneration. (5) Cytosolic cGMP concen-

**TABLE 1.** Time Required for 50% Dephosphorylation of Rho at Specific Sites during Dark Adaptation from Different Bleach Conditions

	50% Dephosphorylation of Rho (h)				
	No Light-Induced Stress	650 lux, 24 h	1300 lux, 24 h	2500 lux, 24 h	5000 lux, 24 h
BN 334 <sup>Ser</sup>	0.15 ± 0.02	0.15 ± 0.02	1.8 ± 0.2	2.5 ± 0.5	3 ± 0.5
BN 338 <sup>Ser</sup>	0.1 ± 0.05	0.1 ± 0.05	0.2 ± 0.04	0.5 ± 0.1	1 ± 0.2
SD 334 <sup>Ser</sup>	2 ± 0.2	2.5 ± 0.3	3.5 ± 0.5	5 ± 0.5	6 ± 0.8
SD 338 <sup>Ser</sup>	0.7 ± 0.1	1.5 ± 0.2	3 ± 0.6	4 ± 0.8	5 ± 0.5
RCS 334 <sup>Ser</sup>	84 ± 12	120 ± 10	168 ± 15	>200	>200
RCS 338 <sup>Ser</sup>	48 ± 10	60 ± 8	72 ± 10	120 ± 15	150 ± 12

BN, SD, or RCS rats treated by light-induced stress with 650, 1300, 2500, or 5000 lux for 24 hours were then kept in the dark. At several time points (up to 400 h), rats were euthanized, and enucleated eyes were processed with immunofluorescence labeling by anti-P-Rho334 or anti-P-Rho338 antibody Rates of dephosphorylation in phosphorylated 334<sup>Ser</sup> and 338<sup>Ser</sup> sites were estimated by plotting of vertical length of the immunofluorescence labeled ROS as described in Figure 5, and time required for 50% dephosphorylation of Rho at specific sites was calculated. For one analysis, three eyes from three rats were used. Experiments were performed on fresh preparations. Data are expressed as the mean ± SD.



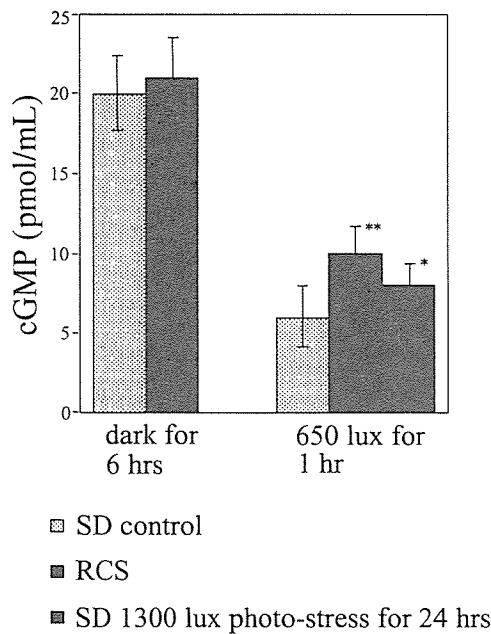


**FIGURE 6.** Retinal cytosolic cGMP concentrations in RCS rats and light-induced stress-treated SD rats. Retinal cytosolic cGMP concentrations were determined by ELISA. Analysis was performed using SD or RCS rats kept under dark for 6 hours and 650 lux light adaptation for 1 hour. In light-induced stress treated SD rat, rats kept at 650 lux light adaptation after light-induced stress (1300 lux) for 24 hours were analyzed. For one analysis, two eyes from one rat were used. Data are expressed as the mean  $\pm$  SD. Experiments were performed in triplicate using fresh preparations. \* $P < 0.05$ , \*\* $P < 0.01$  (Mann-Whitney test).

trations were modulated by light-induced stress. (6) There were no significant changes in expression of the mRNA of several neurotrophic factors, including FGF2, PDGF, and CNTF in the light-induced retinal degeneration model.

In terms of the abnormalities of photoreceptor cells in RCS rats, several changes were noted in the RCS ROS including opsin,<sup>16</sup> arrestin,<sup>17,18</sup> and ROS protein phosphorylation levels,<sup>19</sup> which may affect quenching of the phototransduction pathway. In our previous study in RCS rats compared with SD rats,<sup>20</sup> we performed proteome analysis and found significantly lower levels of expression of the mRNA of  $\alpha$ -A crystalline and rhodopsin kinase (RK), which are thought to be involved in post-Golgi processing of opsin and Rho phosphorylation, respectively. In contrast, expression levels of other major proteins of ROS were almost comparable to those in 3-week-old SD rats according to SDS-PAGE analysis.<sup>20</sup> Therefore, we suggested that the kinetics of Rho phosphorylation and dephosphorylation are specifically affected in RCS rats. Thus, in 3-week-old RCS rats, it is reasonable to think that only the kinetics of Rho dephosphorylation is impaired, whereas the kinetics of Rho regeneration is comparable to wild-type rats in the present study. Our previous study involving the *in vitro* biochemical assay revealed that levels of Rho phosphorylation in 3-week-old RCS rats were slightly lower than those in 3-week-old SD rats, but, in contrast, dephosphorylation of phosphorylated Rho showed much slower kinetics in RCS than in SD rat ROS (3 weeks old). Furthermore, with our recent method of using specific antibodies to Rho phosphorylated at the <sup>334</sup>Ser or <sup>338</sup>Ser sites, which are known to be major phosphorylation sites in Rho *in vivo*,<sup>11,21</sup> we were able to evaluate the kinetics of dephosphorylation of phosphorylated photo-lyzed Rho in RCS and wild-type rats and SD and BN rats *in vivo*. This method applied during dark adaptation showed that de-

phosphorylation of <sup>338</sup>Ser and <sup>334</sup>Ser sites was completed within several hours (0.2–2 hours) in SD and BN rat retinas. However, those antibodies directed toward phosphorylated-<sup>338</sup>Ser and -<sup>334</sup>Ser sites were diminished within 4 to 7 days in RCS rat retinas. Therefore, we hypothesized that extremely prolonged survival of phosphorylated forms of Rho may contribute to persistent misregulation of phototransduction processes in retinal degeneration in RCS rat.<sup>10,22</sup> Our present results suggest that light-induced retinal degeneration may be caused by the same mechanism of RCS rat retinal degeneration as just described. since we found that light-induced stress also caused significant delay in the kinetics of Rho dephosphorylation. Furthermore, the retinal photoreceptor degenerative model of cancer-associated retinopathy (CAR), which is produced by intravitreal administration of anti-recoverin antibody to rats, showed significant high levels of Rho phosphorylation.<sup>23,24</sup> In addition, Rho mutants within the C terminus, in which <sup>345</sup>Val and <sup>347</sup>Pro are the most common sites of mutations causing autosomal dominant retinitis pigmentosa (adRP),<sup>25,26</sup> were also phosphorylated at significantly higher levels than in wild-type.<sup>27</sup> Therefore, prolonged survival of phosphorylated Rho by lower phosphatase activities or enhanced Rho kinase activities may be one of the common mechanisms responsible for most of the retinal photoreceptor degeneration. Although slow kinetics in Rho dephosphorylation was commonly observed in these retinal degenerations, the degree of kinetic change did not correspond to the severity of retinal degeneration. Additional unknown mechanisms must therefore be present to account for retinal degeneration.

As possible events occurred after the prolonged survival of the phosphorylated form of Rho in the light-damaged model, we can suggest the following mechanisms: (1) Phosphorylated Rho continuously suppresses light-dependent transducin activation causing cGMP accumulation within the cytosol; (2) cGMP-gated channels on plasma membranes are continuously open; (3) there is an increase in intracellular  $Ca^{2+}$  levels; and (4) a  $Ca^{2+}$ -dependent apoptotic pathway is activated. In our present study, retinal cytosolic cGMP levels were significantly high in the RCS rat retina and light-induced, stress-treated wild-type retina under light adaptation to 650 lux for 1 hours ( $P < 0.05$ ; Fig. 6). Because it is well known that cytosolic cGMP concentrations were strictly regulated by PDE and guanylate cyclase,<sup>28</sup> despite a relatively small difference as shown in Figure 6, this may induce misregulation of the phototransduction pathway by changing states of cGMP gated channels. This speculated mechanism is almost identical with the molecular pathology of CAR.<sup>3</sup> In the CAR rat model obtained by intravitreal administration of anti-recoverin antibody, the following set of events have been experimentally been determined: (1) anti-recoverin antibody penetrating the photoreceptor cells,<sup>23,29</sup> (2) binding of the anti-recoverin antibody with recoverin, (3) blocking of recoverin function and inhibition of RK in a calcium-dependent manner causing enhancement of Rho phosphorylation,<sup>24</sup> (4) marked suppression of light-dependent transducin activation, (5) continued opening of cGMP gated channels on plasma membranes resulting in an increase of intracellular  $Ca^{2+}$  levels,<sup>30</sup> and (6) activation of the caspase-dependent apoptotic pathway.<sup>23,31</sup> Therefore, an increase of intracellular  $Ca^{2+}$  levels that activate apoptosis is the key mechanism causing both CAR and light-induced retinal degeneration. In fact, our previous study demonstrated that normalization of elevated intracellular  $Ca^{2+}$  levels by nilvadipine, a  $Ca^{2+}$  channel blocker that preferably transfers to central nervous system (CNS), significantly protected against retinal degeneration in light-induced retinal degeneration, RCS,<sup>32</sup> and CAR model rats.<sup>33</sup>

Protective effects toward retinal disease in RCS rats and other retinal degenerations have been demonstrated with me-

chanical damage,<sup>34</sup> laser burns,<sup>35</sup> and light-induced stress.<sup>2</sup> Regarding the possible mechanisms of their retinal protective effects, they commonly induced enhancement of intrinsic neurotrophic factors, such as FGF2. In fact, intravitreal administration of several neurotrophic factors, including FGF2,<sup>36-38</sup> lens epithelium-derived growth factor (LEDGF),<sup>39</sup> and hepatocyte growth factor (HGF)<sup>40</sup> have shown significant protective effects. This mechanism is still the most likely because our previous study demonstrated significant upregulation of FGF2 and Arc during nilvadipine-induced retinal protection of RCS rat retina by DNA microarray analysis.<sup>41</sup> However, in contrast, there were not any significant changes in expression of neurotrophic factors in our present study, including FGF2, PDGF, and CNTF on light-induced stresses to wild-type and RCS rat retinas. It may be speculated that upregulation of neurotrophic factors by the retina within various species could require certain specific conditions of light-induced stress. Evidently, Nir et al.<sup>7,8</sup> described variations over time for the beneficial effects of light-induced stress to RCS rats. They found that the most notable beneficial effects in 23-day-old RCS rats, whereas only a slight effect was detected in 18-day-old rats. In our experiment, 18-day-old RCS rats were exposed to various intensities of light, and retinal morphology was almost normal in light microscopy examination, with slight deterioration of the ERG amplitude. Nevertheless, a light-induced effect on 23-day-old RCS rats could not suitably be evaluated because ERG responses were diminished and retinal morphology had severely deteriorated within 30 days in our RCS rat strain. Another possible reason for the difference in the light-induced effects observed by Nir et al.<sup>7,8</sup> and that in our present study is that the genetic background of the RCS rats may be somewhat different. In addition, in the experimental methods of Nir et al., rats were exposed to bright white light of 110 to 130 ft-c before intense light-induced stress, as a preconditioning protocol. In contrast, in our light-induced stress experiments, no such preconditioning was used. This difference in methods may be an alternative reason for the discrepancy in terms of the neurotrophic factor expression on light-induced stress. Nevertheless, Nir et al. reported that light-induced retinal rescue was found only in the RCS rat but not in the P23H rat, another model of RP.

In conclusion, light-induced stress caused significant delay in the kinetics of Rho dephosphorylation resulting in misregulation of the visual transduction cascade in both normal and RCS retinal degeneration, and light-induced retinal rescue may occur in some specific animal species under certain special conditions.

### Acknowledgements

The authors thank Tadao and Akiko Maeda for excellent editing of the manuscript.

### References

- Soeft SV, Westerveld A, Dejong PTVM, et al. Retinitis pigmentosa: defined from a molecular point of view. *Surv Ophthalmol*. 1999; 43:321-334.
- Wenzel A, Grimm C, Samardzija, Reme, et al. Molecular mechanisms of light-induced photoreceptor apoptosis and neuroprotection for retinal degeneration. *Prog Retinal Eye Res*. 2005;24:275-306.
- Ohguro H, Nakazawa M. Pathological roles of recoverin in cancer-associated retinopathy. In: Palczewski K, Baehr W, eds. *Photoreceptor and Calcium*. New York; Landes Bioscience; 2002;109-124.
- Mullen RJ, LaVail MM. Inherited retinal dystrophy: primary defect in pigment epithelium determined with experimental rat chimeras. *Science*. 1976;201:1023-1025.
- Goldman AI, O'Brien PJ. Phagocytosis in the retinal pigment epithelium of the RCS rat. *Science*. 1978;201:1023-1025.
- Edwards RB, Szamier RB. Defective phagocytosis of isolated rod outer segments by RCS rat retinal pigment epithelium in culture. *Science*. 1977;197:1001.
- Nir I, Liu C, Wen R. Light treatment enhances photoreceptor survival in dystrophic retinas of Royal College of Surgeons rats. *Invest Ophthalmol Vis Sci*. 1999;40:2383-2390.
- Nir I, Harrison JM, Liu C, Wen R. Extended photoreceptor viability by light stress in the RCS rats but not in the opsin P23H mutant rats. *Invest Ophthalmol Vis Sci*. 2001;42:842-849.
- Bush RA, Kononen L, Machida S, et al. The effect of calcium blocker D-cis-diltiazem on photoreceptor degeneration in the rhodopsin Pro23His rat. *Invest Ophthalmol Vis Sci*. 2000;41:2697-2701.
- Ohguro H, Ohguro I, Mamiya K, et al. Prolonged survival of the phosphorylated form of rhodopsin during dark adaptation of royal college surgeons rat. *FEBS Lett*. 2003;551:128-132.
- Ohguro H, Hooser JPV, Milam AH, et al. Rhodopsin phosphorylation and dephosphorylation in vivo. *J Biol Chem*. 1995;270:14259-14262.
- McKechnie NM, Fould WS. Qualitative observation on the variations of light induced damage to rabbit retina. *Graefes Arch Clin Exp Ophthalmol*. 1981;215:305-325.
- Williams TP, Howell WL. Action spectrum of retinal light-damage in albino rats. *Invest Ophthalmol Vis Sci*. 1983;3:285-287.
- Wong P, Kutty RK, Darrow RM, et al. Changes in clusterin expression associated with light-induced retinal damage in rats. *Biochem Cell Biol*. 1994;72:499-503.
- Iseli HP, Wenzel A, Hafezi F, et al. Light damage susceptibility and RPE65 in rats. *Exp Eye Res*. 2002;75:407-413.
- Nir I, Sagie G, Papermaster DS. Opsin accumulation in photoreceptor inner segment plasma membranes of dystrophic RCS rats. *Invest Ophthalmol Vis Sci*. 1987;28:62-69.
- Mirshahi M, Thillaye B, Tarraf M, et al. Light-induced changes in S-antigen (arrestin) localization in retinal photoreceptors: differences between rods and cones and defective process in RCS rat retinal dystrophy. *Eur J Cell Biol*. 1994;63:61-67.
- Clarke IS, Dzialoszynski T, Sanford SE, et al. A possible relationship between cataract, increased levels of the major heat shock protein HSP 70 and decreased levels of S-antigen in the retina of the RCS rat. *Exp Eye Res*. 1991;53:545-548.
- Heth CA, Schmidt SY. Protein phosphorylation in retinal pigment epithelium of Long-Evans and Royal College of Surgeons rats. *Invest Ophthalmol Vis Sci*. 1992;33:2839-2847.
- Maeda A, Ohguro H, Maeda T, et al. Low expression of  $\alpha$ -crystalline and rhodopsin kinase of photoreceptors in retinal dystrophy rat. *Invest Ophthalmol Vis Sci*. 1999;40:2788-2794.
- Kennedy MJ, Lee KA, Niemi GA, et al. Multiple phosphorylation of rhodopsin and the in vivo chemistry underlying rod photoreceptor dark adaptation. *Neuron*. 2001;31:87-101.
- Ohguro H, Ohguro I, Nakazawa M. Role of rhodopsin phosphorylation at multiple sites in vivo. *Hiroaki Med J*. 2005;56:61-68.
- Ohguro H, Ogawa K, Maeda T, et al. Cancer-associated retinopathy induced by both anti-recoverin and anti-hsc70 antibodies in vivo. *Invest Ophthalmol Vis Sci*. 1999;40:3160-3167.
- Maeda T, Maeda A, Maruyama I, et al. Mechanisms of photoreceptor cell death in cancer-associated retinopathy. *Invest Ophthalmol Vis Sci*. 2001;42:705-712.
- Dryja TD. Rhodopsin and autosomal dominant retinitis pigmentosa. *Eye*. 1992;6:1-10.
- Nakazawa M, Kikawa-Araki E, Shiono T, et al. Analysis of rhodopsin gene in patients with retinitis pigmentosa using allele-specific polymerase chain reaction. *Jpn J Ophthalmol*. 1991;35:386-393.
- Ohguro H. High levels of rhodopsin phosphorylation in missense mutations of C-terminal region of rhodopsin. *FEBS Lett*. 1997;413:433-435.
- Palczewski W, Sokal I, Baehr W. Guanylate cyclase-activating proteins: structure, function and diversity. *Biochem Biophys Res Commun*. 2004;322:1123-1130.

29. Adamus G, Machnicki M, Seigel GM. Apoptotic retinal cell death induced by antirecoverin autoantibodies of cancer-associated retinopathy. *Invest Ophthalmol Vis Sci.* 1997;38:283-291.
30. Adamus G, Webb S, Shiraga S, et al. Anti-recoverin antibodies induce an increase in intracellular calcium, leading to apoptosis in retinal cells. *J Autoimmun.* 2006;26:146-153.
31. Adamus G, Machnicki M, Elerding H, et al. Antibodies to recoverin induce apoptosis of photoreceptor and bipolar cell in vivo. *J Autoimmun.* 1998;33:523-533.
32. Ohguro H, Ogawa K, Maeda T, et al. Retinal dysfunction in cancer-associated retinopathy is improved by  $Ca^{2+}$  antagonist administration and dark adaptation. *Invest Ophthalmol Vis Sci.* 2001;42:2589-2595.
33. Yamazaki H, Ohguro H, Maeda T, et al. Nilvadipine, a  $Ca^{2+}$  antagonist, effectively preserves retinal morphology and functions in Royal College of Surgeons rat. *Invest Ophthalmol Vis Sci.* 2002;43:919-926.
34. Silverman MS, Hughes SE. Photoreceptor rescue in the RCS rat without pigment epithelium transplantation. *Curr Eye Res.* 1990;9:183-191.
35. Xiao M, Sastry SM, Li ZY, et al. Effects of retinal laser photocoagulation on photoreceptor basic fibroblast growth factor and survival. *Invest Ophthalmol Vis Sci.* 1998;39:618-630.
36. Faktorovich EG, Steinberg RH, Yasumura D, et al. Photoreceptor degeneration in inherited retinal dystrophy delayed by basic fibroblast growth factor. *Nature.* 1990;347:83-86.
37. Faktorovich EG, Steinberg RH, Yasumura D, et al. Basic fibroblast growth factor and local injury protect photoreceptors from light damage in the rat. *J Neurosci.* 1992;12:3554-3567.
38. Perry J, Du J, Kjeldbye H, Gouras P. The effects of bFGF on RCS rat eyes. *Curr Eye Res.* 1995;14:585-592.
39. Machida S, Chaudhry P, Shinohara T, et al. Lens epithelium-derived growth factor promotes photoreceptor survival in light-damaged and RCS rats. *Invest Ophthalmol Vis Sci.* 2001;42:1087-1095.
40. Machida S, Tanaka M, Ishii T, et al. Neuroprotective effect of hepatocyte growth factor against photoreceptor degeneration in rats. *Invest Ophthalmol Vis Sci.* 2004;45:4174-4182.
41. Sato M, Ohguro H, Ohguro I, et al. Study of pharmacological effects of nilvadipine on RCS rat retinal degeneration by microarray analysis. *Biochem Biophys Res Commun.* 2003;306:826-831.

## 48. フーリエドメイン OCT による網膜色素変性の網膜 3 次元解析

川越直顕<sup>1)</sup>、板谷正紀<sup>1)</sup>、大石明生<sup>1)</sup>、坂本 篤、秋元正行<sup>1)</sup>  
大谷篤史<sup>1)</sup>、高橋政代<sup>1)</sup>、吉村長久<sup>1)</sup>、安野嘉晃<sup>2)</sup>、巻田修一<sup>2)</sup>  
(<sup>1)</sup>京都大、<sup>2)</sup>筑波大)

**研究要旨** Stratus OCT により黄斑部視細胞内節外節の境界部 (IS/OS) の所見が網膜色素変性 (RP) の視機能障害の程度を反映すると報告されている。Stratus OCT よりも高速かつ高感度なフーリエドメイン光干渉断層計 (FD-OCT) による RP の黄斑部網膜所見を Stratus OCT と比較した。二次元画像においては IS/OS の残存の程度がより明確に観察された。3 次元観察により、残存 IS/OS の範囲を観察することが可能であった。ELM ラインと色素上皮ラインの間隔を観察することで、視細胞内節外節の様々な程度の菲薄化を評価することができた。CME と ERM も 3 次元的に描出することにより病変を立体的に捉える事ができた。

**【結論】** FD-OCT は従来の OCT に比べて網膜色素変性の視細胞層の描出能力に優れており、視細胞層の菲薄化や CME、ERM などの病変を早期に観察する事が可能である。さらに三次元画像解析によりその範囲を捉えることが可能であり、かつ病変を立体的に観察する事も可能である。

### A. 研究目的

Stratus OCT により黄斑部視細胞内節外節の境界部 (IS/OS) の所見が網膜色素変性 (RP) の視機能障害の程度を反映すると報告されている。Stratus OCT よりも高速かつ高感度なフーリエドメイン光干渉断層計 (FD-OCT) による RP の黄斑部網膜所見を Stratus OCT と比較し報告する。

### B. 研究方法

トプコン社製無散瞳カメラに組み込んだ FD-OCT を用いて黄斑部を中心とした 2.8mm × 2.8mm の領域で 256 x 256 のラスタスキャンを行い 2 次元画像を取得し網膜構造を解析した。さらに連続する二次元画像を 2 5 6 枚重ね合わせて 3 次元画像を構築し立体的な構造を観察した。

### (倫理面への配慮)

非侵襲的検査である。

### C. 研究結果

二次元画像においては、全症例において IS/OS に相当する後方反射ラインが Stratus OCT よりも明瞭に認められた。その結果、IS/OS の残存の程度がより明確に観察された。さらに 3 次元観察により、残存 IS/OS の範囲を観察することが可能であった。Stratus OCT では不明瞭であった外境界膜 (ELM) に相当するラインが 20 例中 16 眼で明瞭に観察された。ELM ラインと色素上皮ラインの間隔を観察することで、視細胞内節外節の様々な程度の菲薄化を評価することができた。CME と ERM も 3 次元的に描出することにより病変を立体的に捉

える事ができた。

#### D. 考察

網膜色素変性の病状の進行により視細胞内節外節が菲薄化すると同時に範囲も狭小化していくと考えられる。

#### E. 結論

FD-OCT は従来の OCT に比べて網膜色素変性の視細胞層の描出能力に優れており、視細胞層の菲薄化や CME、ERM などの病変を早期に観察する事が可能である。さらに三次元画像解析によりその範囲を捉えることが可能であり、かつ病変を立体的に観察する事も可能である。

F. 健康危険情報           なし

#### G. 研究発表

1. 論文発表               なし

2. 学会発表

フーリエドメイン光干渉断層計による  
網膜色素変性における黄斑部の観察  
第 60 回日本臨床眼科学会

#### H. 知的財産権の出願・登録状況

1. 特許取得               なし

2. 実用新案登録       なし

3. その他               なし

#### I. 参考文献

B Sander, al et: Enhanced optical coherence tomography imaging by multiple scan averaging. Br J Ophthalmol. 89 :207-212, 2005.

## 49. 超音波とバブルリポソームを利用した

### 培養角膜上皮細胞およびラット結膜への遺伝子導入

山下敏史<sup>1)</sup>、園田祥三<sup>1)</sup>、立花克郎<sup>2)</sup>、鈴木 亮<sup>3)</sup>、丸山一雄<sup>3)</sup>、坂本泰二<sup>1)</sup>

(<sup>1)</sup>鹿児島大、<sup>2)</sup>福岡大解剖学、<sup>3)</sup>帝京大薬学部生物薬剤)

**研究要旨** 遺伝子導入法の一つとして、超音波 (US) とバブル製剤を併用した方法が注目されている。昨年、マイクロバブル併用超音波遺伝子導入法の眼球への応用について報告した。今回は、新しいバブル製剤であるバブルリポソームを併用した超音波遺伝子導入法の眼球での検討を行った。

*In vitro*: ラット培養角膜上皮細胞を対象に、発現したGreen fluorescent protein (GFP) プラスミドのカウントにより導入効率を評価した。至適条件でのBL併用超音波照射群では、細胞毒性もなく、MB併用超音波照射と比べ、より少ない照射時間でより効率的な遺伝子導入効率が可能であった。

*In vivo*: ラット上眼瞼結膜を対象に、発現したGFP プラスミドのスコア分類により導入効率を評価した。BL併用超音波照射群では、有意に導入効率が向上した。組織標本でも、GFP蛍光が観察され、明らかな組織障害は認められなかった。

BL併用超音波遺伝子導入法は、眼球へ利用可能であり、治療法としての可能性がある。

#### A. 研究目的

超音波遺伝子導入法の際、マイクロバブル (MB) を併用すると、導入効率が向上する。昨年、この方法の眼球への応用について報告した。最近になり、新しいバブル製剤であるバブルリポソーム (BL) を発案し、今回、この BL 併用超音波遺伝子導入法の眼球での検討を行った。

#### B. 研究方法

BL は、内部にガスをもつナノサイズの泡で、MB の数 10 分の一の大きさである。また、付加されている Polyethyreneglycol (以下 PEG と略す) によって血中での安定性に優れているとともに、様々な分子をリガンド

することが可能である。

*In vitro*: ラット培養角膜上皮細胞 (RC-1) を培養皿に調整し、GFP プラスミドと BL の混合液を添加後、US 照射装置 (ソニトロン 2000) を用いて、各種条件で照射した (n=43)。US照射単独群 (n=15)、MB併用US照射群 (n=15) にも同様の実験を行った。48 時間後に蛍光倒立顕微鏡を使って導入効率を判定し、MTS-assay を用いて細胞障害性を判定した。

*In vivo*: ラットの上眼瞼結膜下に、GFP プラスミドと BL の混合液を注射後、US 照射した。プラスミド注射群、プラスミド+ US照射群を対象とし同様に実験を行った (各群、n=10)。実体顕微鏡で導入効率を判定

し、摘出標本で細胞障害の有無とGFP蛍光を検討した。

#### (倫理面への配慮)

動物実験は、鹿児島大学動物実験倫理規定に従って実験を行った。

### C. 研究結果

#### *In vitro*

BL 併用超音波照射群においては、各条件で、10%以上の遺伝子導入が可能だったが、指摘条件（超音波パワー1.2W/cm<sup>2</sup>、照射時間 20 秒、BL; 21 μg/well）の群では、約 27%と有意に導入効率が向上した（p<0.05: ANNOVA test）。至適条件での導入効率と、コントロール群、超音波単独照射群、MB 併用超音波照射群での導入効率を比較すると、BL 併用超音波照射群では、他群と比べ導入効率が有意に向上していた（p<0.01: unpaired-T test）。また、BL 併用群での照射時間を比較すると、60 秒よりも 20 秒の方が導入効率が向上していた（p<0.01: unpaired-T test）。MTS-assay では明らかな細胞毒性は認められなかった。



写真1 至適条件下での蛍光顕微鏡写真

#### *In vivo*

混合液注射のみの群、超音波単独照射群でも遺伝子導入は可能だったが、BL 併用群では、有意に遺伝子導入効率が向上した。組織標本では、明らかな障害は観察されず、GFP 蛍光が結膜粘膜固有層に認められた。

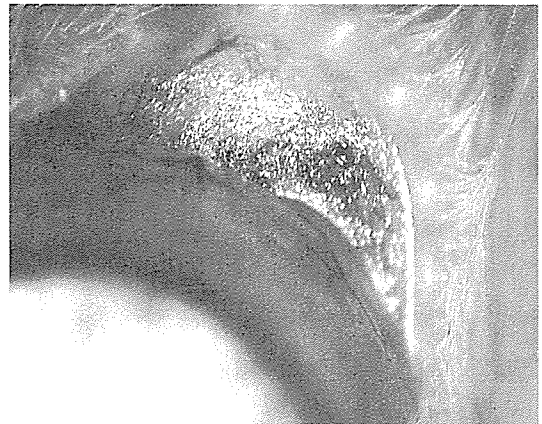


写真2 結膜のGFP 蛍光（実体顕微鏡）

### D. 考察

BL 併用超音波遺伝子導入法は、安全かつ効率的な遺伝子導入ができる方法であり、眼科領域での応用が可能だった。今後、網膜や視神経などの他の部位への遺伝子導入、BL の特性を生かしたドラッグデリバリーへの応用など、大きな可能性を持っている。

### E. 結論

BL 併用超音波遺伝子導入法は、眼球へも応用可能である。遺伝子治療やドラッグデリバリーとして、新しい治療法の開発につながる可能性がある。

F. 健康危険情報           なし

### G. 研究発表

1. 論文発表               なし

## 2. 学会発表 (予定)

1. 山下敏史 他: 超音波とバブルリソームを利用した培養角膜上皮細胞およびラット結膜への遺伝子導入. 第 111 回日本眼科学会総会、大阪、2007
2. Toshifumi Y et al: Gene delivery by combination of bubble liposome and ultrasound for corneal epithelial cells. The Association for Research in Vision and Ophthalmology (ARVO), Fort Lauderdale, Florida, 2007
5. Shozo Sonoda et al. Gene transfer to corneal epithelium and keratocyte mediated by ultrasound with microbubbles. IOVS 47: 558-564, 2006.
6. Suzuki et al: Gene delivery by combination of novel liposomal bubbles with perfluoropropan and ultrasound. J Cont. Release (in press)

## H. 知的財産権の出願・登録状況

1. 特許取得                   なし
2. 実用新案登録           なし
3. その他                    なし

## I. 参考文献

1. Tachibana K et al: InInduction of cell-membrane porosity by ultrasound. Lancet 353: 1409, 1999.
2. Sakamoto T et al: Target gene transfer of tissue plasminogen activator to cornea by electric pulse inhibits intracameral fibrin formation and corneal cloudiness. Hum Gene Ther 10: 2551-2557, 1999.
3. Taniyama Y et al: Development of safe and efficient novel nonviral gene transfer using ultrasound: enhancement of transfection efficiency of naked plasmid DNA in skeletal muscle. Gene Ther 9: 372-380, 2002.
4. Marshall E. Gene therapy's growing pains. Science 269: 1050,



## 50. 硝子体手術併用眼内超音波遺伝子導入法の開発

園田祥三<sup>1)</sup>、内野英輔<sup>1)</sup>、坂本泰二<sup>1)</sup>、鈴木 亮<sup>2)</sup>、丸山一雄<sup>2)</sup>、立花克郎<sup>3)</sup>

(<sup>1)</sup>鹿児島大、<sup>2)</sup>帝京大薬学部生物薬剤教室、<sup>3)</sup>福岡大医学部解剖学)

**研究要旨** 我々が研究を続けている超音波やマイクロバブル(以下MB)を組み合わせた遺伝子導入法について、新たな眼球への超音波照射方法を考案し効果を検討した。兎硝子体を25G システムを使って切除後、硝子体腔内に超音波プローブを挿入した状態で、Green Fluorescent Protein (GFP) プラスミド・バブル混合液を注入しながら超音波を網膜へ照射した。48時間後に眼球を摘出し、蛍光顕微鏡で観察を行うと、網膜視細胞層を中心に GFP 蛍光が観察できた。処置中および処置後も眼球に異常は認めず、H.E 染色で組織障害はなかった。硝子体手術併用眼内超音波遺伝子導入法は、今後応用の可能性が期待できる。

### A. 研究目的

我々は、超音波とマイクロバブル (MB) を利用した眼球への遺伝子導入法 sonoporation に有用性について報告した (Sonoda et al. *IOVS* 2006)。今回、MB にかわって新素材バブルリポソーム (BL) を併用した遺伝子導入法について、ラット結膜を用いたモデルで検討を行い本会で報告を行っている。本研究では BL 併用下に、網膜への新しい超音波照射法による遺伝子導入方法について検討した。

### B. 研究方法

超音波照射装置 Sonopore4000™ を使用し、照射プローブは血管内超音波照射用として用いられている Ultrasound Thrombolytic Infusion Catheter™ (EKOS Corporation) を利用した。白色家兎眼球を用い、Alcon 社 25G システムを使って硝子体切除を行った後、超音波プローブを強膜ポートから硝子体内に挿入、27G 針をつかってトロカール経由で硝子体内に Green Fluorescent

Protein (GFP) プラスミド・BL 混合液 (1:1, 計 60 $\mu$ L) を注入しながら、超音波を照射した (1MHz, 1W/cm<sup>2</sup>, duty 比 7%, 60 秒)。対象として、無処置群、プラスミド注射単独群 (硝子体切除、非切除群)、プラスミド・超音波併用群でも同様の実験を行った。実験終了 48 時間後に、細隙灯検査、眼底検査を行った後、眼球を摘出し凍結切片を作成した。蛍光顕微鏡をつかって GFP を観察し遺伝子導入の有無を検討した。併せて H.E. 染色を行い、組織障害の有無についても検討した。

### (倫理面への配慮)

動物実験は、鹿児島大学動物実験倫理規定に従って実験を行った。

### C. 研究結果

25G システムを使うことによって眼球は安定し、眼内で超音波の照射中特に問題はなかった。超音波プローブもスムーズに毛様体部からの出し入れが可能であった。眼球摘出時、前眼部、眼底に明らかな異常は認

めなかった。摘出眼球の組織学検査ではすべての群で明らかな異常はなかった。GFP 蛍光陽性細胞は、BL・超音波併用群のみで観察可能で、網膜視細胞を中心に陽性細胞が存在していた。

#### D. 考察

硝子体腔内で超音波を照射するという新しい概念は今後新たな治療法の開発につながる可能性がある。眼内で安全に超音波を照射するために新たな照射プローブの開発が不可欠である。

#### E. 結論

眼内にプローブを直接挿入し、安全に超音波を照射することが可能であり、これらの方法は今後あらたな眼内への遺伝子導入法の開発につながる可能性がある。

F. 健康危険情報                   なし

#### G. 研究発表

##### 1. 論文発表

1. Shozo Sonoda et al: Gene transfer to corneal epithelium and keratocyte mediated by ultrasound with microbubbles, IOVS 47:558-564, 2006.
2. 園田祥三: ドラッグデリバリーシステム、超音波とマイクロバブル(MB)を用いたドラッグデリバリーシステム 眼薬理学会雑誌 20: 19-40, 2006.

##### 2. 学会発表

1. 園田祥三 他: 眼瞼メラノーマに対する超音波とマイクロバブル併用時のブレオマイシンの抗腫瘍効果の検討、

第2回 ソノポレーション研究会、福岡, 2006.

2. 園田祥三、坂本泰二、超音波とマイクロバブルを用いたラット網膜への遺伝子導入、日本眼科学会専門別研究会、京都, 2006.
3. Shozo Sonoda et al.: Ultrasound-mediated gene transfer into rat retina using micro-bubbles, ARVO, FL, 2006

#### H. 知的財産権の出願・登録状況

##### 1. 特許取得(出願中)

眼球組織への生理活性薬剤導入のための組成物および装置。

出願番号 特許 2005-221346

2. 実用新案登録                   なし
3. その他                           なし

##### 1. 参考文献

1. Tachibana K et al: Induction of cell-membrane porosity by ultrasound. Lancet 353: 1409, 1999.
2. Suzuki R et al: Gene deliver by combination of novel bubbles with perfluoropropane and ultrasound.
3. Sakamoto T et al: Target gene transfer of tissue plasminogen activator to cornea by electric pulse inhibits intracameral fibrin formation and corneal cloudiness. Hum Gene Ther 10: 2551-2557, 1999
4. Taniyama Y et al: Development of safe and efficient novel nonviral gene transfer using ultrasound:

enhancement of transfection  
efficiency of naked plasmid DNA in  
skeletal muscle. *Gene Ther* 9:  
372-380, 2002.

## 51. 全膜蛋白欠損型センドイウイルスベクターの

### 網膜への遺伝子導入特性に関する検討

村上祐介<sup>1,2)</sup>、池田康博<sup>2)</sup>、米満吉和<sup>3)</sup>、岡野慎士<sup>1)</sup>、向野利一郎<sup>2)</sup>

宮崎勝徳<sup>2)</sup>、井上 誠<sup>4)</sup>、長谷川護<sup>4)</sup>、石橋達朗<sup>2)</sup>、居石克夫<sup>1)</sup>

(<sup>1)</sup>九州大病理病態学、<sup>2)</sup>九州大、<sup>3)</sup>千葉大遺伝子治療学、<sup>4)</sup>DNAVEC(株)

**研究要旨** センドイウイルス(SeV)ベクターは、高い遺伝子導入効率と安全性を併せ持つ国産遺伝子導入ベクターとして、慢性重症虚血肢に対し既に臨床応用が開始されている。網膜では、網膜下投与により網膜色素上皮細胞への効率的な遺伝子導入が可能だが、導入後の炎症に伴う組織傷害が問題であった。今回我々は SeV の免疫応答に関与する膜蛋白遺伝子(F,M,HN)をすべて欠損させた 3 欠損型 SeV ベクター (rSeV/dFdMdHN) を用い、網膜での遺伝子導入特性を検討した。3 欠損型 SeV ベクターは F 欠損型に比し、遺伝子発現は同等だったが、組織学的に網膜への炎症細胞浸潤が少なく組織傷害が減弱していた。また炎症性サイトカイン・NK 活性の低下を認め、初期免疫応答の減弱が示唆された。しかし 3 欠損型を用いても SeV 特異的 CTL 活性・抗体価は上昇し、導入後 14 日目には遺伝子発現は消失した。以上の結果より、SeV 膜蛋白は自然免疫応答に深く寄与し、3 欠損型 SeV ベクターを用いることで遺伝子導入後の組織傷害が軽減されることが示された。一方、網膜における遺伝子の長期発現には、獲得免疫の制御が重要と考えられた。

#### A. 研究目的

SeV ベクターは、高い遺伝子導入効率と安全性を併せ持つ国産遺伝子導入ベクターであるが、網膜では導入後の炎症に伴う組織傷害が問題であった。今回我々は SeV の免疫応答に関与する全膜蛋白遺伝子(F,M,HN)を欠損させた 3 欠損型 SeV ベクターを用い、網膜での遺伝子導入特性を検討した。

#### B. 研究方法

GFP、Luciferase を搭載した SeV ベクター (F 欠損型、3 欠損型)溶液を Wistar rat の網膜下に注入し、遺伝子発現を確認した。組

織像、炎症性サイトカイン、NK 活性、CTL 活性、抗体価を検討し、両ベクターの網膜における炎症反応を経時的に比較した。

#### (倫理面への配慮)

実験は当該施設の動物実験委員会の承認を得た後に Association for Research in Vision and Ophthalmology (ARVO)の規定に従って行った。動物の苦痛は最小限となるよう配慮した。

#### C. 研究結果

3 欠損型組換え SeV ベクター遺伝子発現は、F 欠損型と同等であった。組織学的には、F 欠損型では導入網膜への強い炎症細胞浸